Functional consequences of a domain 1/S6 segment sodium channel mutation associated with painful congenital myotonia

Dao W. Wang[a], Dorothy VanDeCarr[a], Peter C. Ruben[b], Alfred L. George Jr.[a,*], Paul B. Bennett[1,a]

[a] *Departments of Pharmacology and Medicine, Vanderbilt University Medical Center, Nashville, TN 37232, USA*
[b] *Department of Biology, Utah State University, Logan, UT 84322, USA*

Received 19 January 1999; received in revised form 2 March 1999

Abstract An unusual form of painful congenital myotonia is associated with a novel *SCN4A* mutation causing a valine to methionine substitution in the domain 1/S6 segment of the skeletal muscle sodium channel. We studied the functional characteristics of this mutant allele using a recombinant channel to gain understanding about the nature of the biophysical defect responsible for this unique phenotype. When expressed heterologously in a cultured mammalian cell line (tsA201), the mutant channel exhibits subtle defects in its gating properties similar, but not identical, to other myotonia-producing sodium channel mutations. The main abnormalities are the presence of a small non-inactivating current that occurs during short test depolarizations, a shift in the voltage-dependence of channel activation to more negative potentials, and a slowing of the time course of recovery from inactivation. Flecainide, a potent sodium channel blocker previously reported to benefit patients affected by this form of myotonia, effectively inhibits the abnormal sodium current associated with expression of the mutant channel. Our findings demonstrate the unique pattern of sodium channel dysfunction associated with a D1/S6 myotonia-producing sodium channel mutation, and provide a mechanism for the beneficial effects of flecainide in this setting.

Key words: Myotonia; Sodium channel; SCN4A; Flecainide

1. Introduction

A variety of inherited syndromes have been linked to mutations in voltage-gated sodium channels [1–3]. Mutations in the skeletal muscle sodium channel α-subunit gene (*SCN4A*, 17q) cause various forms of non-dystrophic myotonia and periodic paralysis [4]. To date, there have been approximately 20 *SCN4A* mutations reported with the majority resulting in amino acid substitutions within the third or fourth repeat domains of the channel [5]. Interestingly, there has been a conspicuous absence of mutations in the first repeat domain (D1) fueling speculation that mutations in this region of a voltage-gated sodium channel would either be inconsequential or possibly lethal.

We recently reported the discovery of the first known sodium channel D1 mutation, a valine to methionine substitution in the D1/S6 segment (V445M), in an unusual form of painful congenital myotonia [6]. The phenotype associated with this mutation is sufficiently distinct from other inherited disorders of muscle membrane excitability associated with *SCN4A* mutations (paramyotonia congenita, hyperkalemic periodic paralysis, and potassium aggravated myotonia) that we postulated it might be associated with a unique pattern of sodium channel dysfunction. We have now characterized this mutation using heterologous expression of recombinant mutant and wild-type (WT) skeletal muscle sodium channel α subunits (hSkM1). Our findings established that the mutation causes a defect in sodium channel gating that is compatible with a myotonia-producing lesion. The pattern of dysfunction is distinct from other muscle sodium channel mutations and this observation supports the notion that D1 sodium channel mutations may be associated with unusual phenotypes. We also demonstrated that flecainide effectively suppressed the abnormal channel behavior consistent with the drug's observed clinical efficacy in treating the associated unusual form of myotonia.

2. Materials and methods

2.1. Site-directed mutagenesis

Valine-445 was replaced by methionine in the hSkM1 cDNA [7] using a cassette mutagenesis strategy. Two complementary oligonucleotides were synthesized and annealed together to form a 70 base pair product containing the mutation, as well as *Hin*DIII and *Sfi*I compatible overhangs. The double-stranded cassette sequence was also designed to eliminate a nearby *Sfi*I recognition site by a silent mutation for use as an allele-specific marker. The double-stranded mutant cassette was phosphorylated using T4 polynucleotide kinase and subcloned into the *Hin*DIII and *Sfi*I sites of a modified hSkM1 cDNA (hSkM1-A) [8] in the mammalian expression plasmid pRcCMV. Recombinants were analyzed by restriction digestion and sequenced fully in the region containing the mutant cassette.

2.2. Expression of sodium channels in tsA201 cells

Transfection-quality plasmid DNA was prepared using the Qiagen method. Cultured tsA201 cells were grown and transiently transfected as previously described [9]. Transiently transfected cells were examined 48 h after transfection following mechanical dissociation from the culture dish.

2.3. Electrophysiology

Sodium channel expression was examined using the whole cell configuration of the patch clamp technique, as previously described [9]. All measurements were made using the pCLAMP suite of programs and analyzed as previously described [9]. The time course of sodium current inactivation was quantified by fitting the falling phase of each current tracing with exponential functions: V445M required a two exponential function, $y = A^1 \cdot \exp(-t/\tau_1) + A^2 \cdot \exp(-t/\tau_2) + C$, whereas hSkM1 data required a single exponential function, $y = A^1 \cdot \exp(-t/\tau_1) + C$, where A is the amplitude of the current component, τ is a time

*Corresponding author. S-3223 MCN, Vanderbilt University Medical Center, 1161 21st Avenue South, Nashville, TN 37232-2372, USA.
Fax: +1 (615) 936-2661.
E-mail: al.george@mcmail.vanderbilt.edu

[1] Present address: MRL, Pharmacology WP26-265, 770 Sumneytown Pike, West Point, PA 19486.

PII: S0014-5793(99)00338-5

constant, and C represents the amount of non-inactivating current. Recovery from inactivation was assessed by a standard two-pulse protocol. Channels were inactivated by a 500 ms prepulse to +20 mV. The fraction of channels that had recovered following various time intervals at −120 mV was calculated by dividing the peak current measured during a subsequent test pulse to −20 mV by the current measured (at −20 mV) after clamping the cell for 10 s at −120 mV. A two-pulse protocol was used to assess the voltage-dependence of steady-state inactivation using a 500 ms prepulse to different membrane potentials. The fraction of channels not inactivated by the prepulse was estimated from the peak inward current during a 20 ms test potential to −20 mV. The voltage-dependence of channel activation was assessed by measuring peak sodium current at different test potentials. Peak sodium current values were divided by the electrochemical driving force ($E_M - E_{Na}$) and normalized to the maximum value measured at +20 mV.

2.4. Computer simulations of muscle action potentials

Sarcolemmal action potentials were simulated using a modified Hodgkin–Huxley mathematical model as previously described [10]. Parameters were changed to simulate the behavior of a 1:1 mixture of WT and mutant sodium channels as would exist in a heterozygous muscle fiber. A slow component of inactivation was included in the mutant simulations using a relative rate constant of 0.15. Also, to simulate the slower time course of recovery from inactivation observed with V445M, the rate constants for fast and slow components of inactivation recovery were multiplied by 0.67 and 0.296, respectively. Simulated action potentials were elicited by a 20 ms, 160 μA/cm^2 stimulus at 37°C.

3. Results and discussion

3.1. Functional properties of V445M

We performed experiments to examine the general functional properties of V445M transiently expressed in tsA201 cells. Fig. 1 illustrates representative whole cell current recordings from cells transfected with either wild-type (WT) or mutant (V445M) hSkM1 cDNA. Sodium currents were elicited by a series of test depolarizations from a holding potential of −120 mV. Expression of both WT and mutant channels was equally robust and there was no significant difference between the recorded peak current amplitudes. There were no readily apparent differences in the time course of either activation or inactivation of the whole cell current traces shown in Fig. 1A and B, however, mutant channels exhibit a small (1–2% of peak current) persistent current during the late phase of the test depolarization. This late current component is illustrated more clearly by the Fig. 1B inset showing superimposed, normalized current recordings in response to a −20 mV test depolarization. Sodium currents recorded in cells transfected with V445M do inactivate fully during longer (100 ms) test depolarizations (data not shown). Current-voltage relationships for WT and mutant channels are illustrated in Fig. 1C and D. The midpoint of the descending limb of the current-voltage relationship and the voltage producing peak current amplitude appear shifted to more negative potentials in the mutant (compared with WT) suggesting that there may be changes in the voltage-dependence of channel gating (see below).

The time course of inactivation was quantified by fitting the data shown in Fig. 1A and B with exponential functions. The time course of current decay in cells transfected with WT-hSkM1 could be well fit with a single exponential function, but the time course of inactivation in cells transfected with V445M required a two exponential fit. Fig. 2 illustrates the voltage-dependence of inactivation time constants for both WT and mutant channels. The time constants for WT inactivation are similar to the fast component of the mutant, but V445M channels exhibit additional slow and late current components. These data illustrate a defect in fast inactivation exhibited by the mutant channel. The time course of recovery from inactivation was also determined and is illustrated in Fig. 2C. By contrast to many other myotonia-producing sodium channel mutations that accelerate the time course of recovery from inactivation [11–13], the V445M allele appears

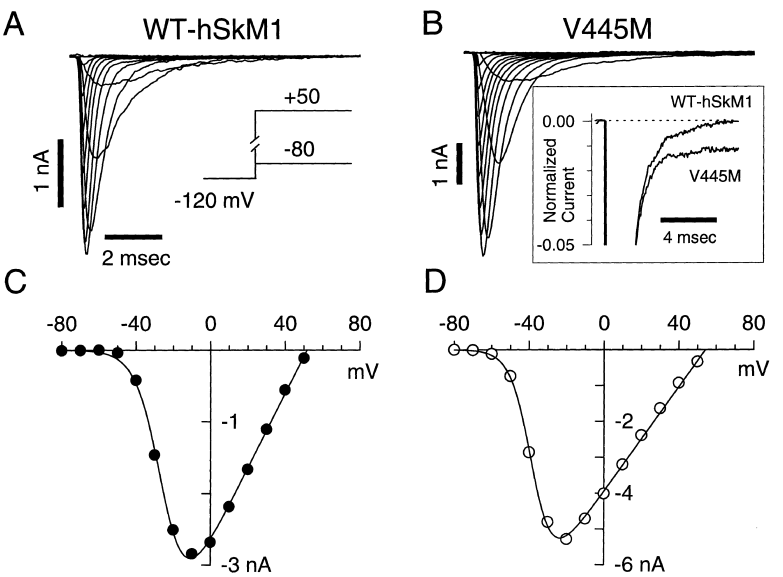

Fig. 1. Current-voltage relationships for WT hSkM1 and V445M. A: Whole cell currents recorded from tsA201 cells expressing WT-hSkM1 elicited by a series of test potentials between −80 mV and +50 mV from a holding potential of −120 mV. B: Currents recorded from tsA201 cells expressing WT-hSkM1 elicited with the same protocol as in panel A. Inset shows normalized current records obtained with a test depolarization to −20 mV on an expanded scale to illustrate the non-inactivating current. C, D: Peak inward current plotted as a function of membrane potential for hSkM1 (C) or V445M (D). Solid curves through data points in C and D were generated by the equation: $I_{Na} = g_{Na} \cdot [1+\exp(V_m - V_{1/2})/k]^{-1} \cdot [V_m - E_{Na}]$. The midpoint values ($V_{1/2}$) for the descending limb of the two curves were −25 and −38 mV for hSkM1 and V445M, respectively.

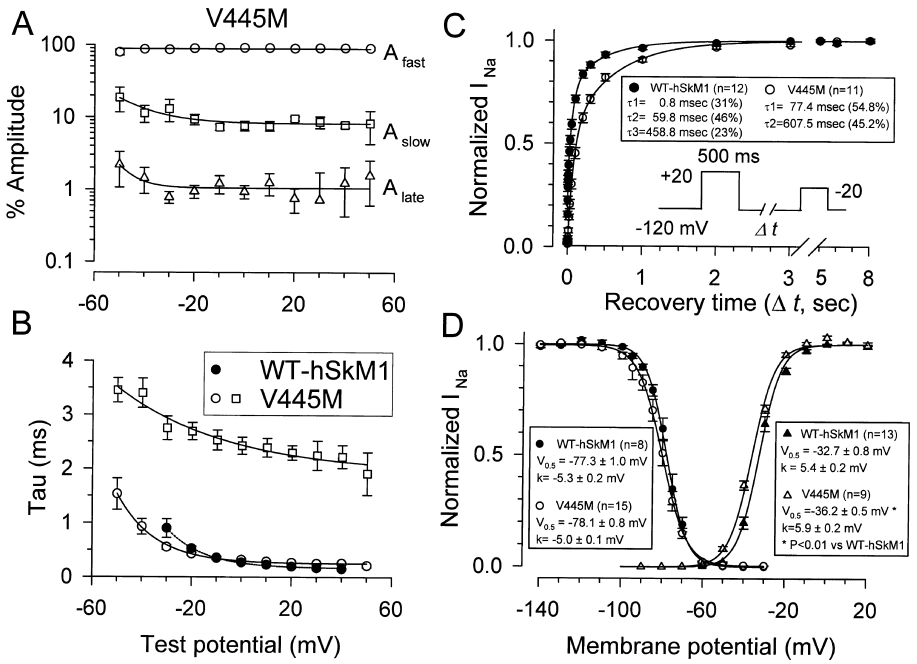

Fig. 2. Quantitative analyses of WT-hSkM1 and V445M gating. A: Relative amplitudes of the fast (○), slow (□), and late (△) inactivating current components observed for V445M. B: Inactivation time constants for hSkM1 and V445M (symbols defined in the inset legend). V445M currents required a two exponential fit thus giving two time constants. C: Recovery from inactivation for WT-hSkM1 and V445M. The best fitting exponential functions for WT-hSkM1 (three components) and V445M (two components) are shown as solid lines obtained from the averaged data. Time constants are as follows (component amplitudes are in parentheses): WT-hSkM1: $\tau_1 = 0.8$ ms (31%), $\tau_2 = 59.8$ ms (46%), $\tau_3 = 459$ ms (23%); V445M: $\tau_1 = 77.4$ ms (54.8%), $\tau_2 = 607.5$ ms (45.2%). D: Comparison of steady-state inactivation (circles) and activation (triangles) curves for WT-hSkM1 (filled symbols) and V445M (open symbols). The curves shown are normalized to the maximum sodium conductance in each experiment and fitted with Boltzmann functions. Values for half-maximal inactivation ($V_{0.5}$) are as follows: WT-hSkM1, -77.3 ± 1.0 mV ($n = 8$); V445M, -78.1 ± 0.8 mV ($n = 15$) (NS). Values for half-maximal activation are as follows: WT-hSkM1, -32.7 ± 0.8 mV ($n = 13$); V445M, -36.2 ± 0.5 mV ($n = 9$) ($P < 0.01$).

to produce slowing of this process. It is difficult to compare the time course of recovery from inactivation for WT and V445M quantitatively because of a difference in the number of exponential components required for fitting these curves. Steady-state inactivation and conductance vs. voltage plots are shown in Fig. 2D for both WT and mutant channels. There is no significant difference in steady-state inactivation between the two channel alleles. However, the voltage-dependence of activation is shifted significantly to more negative potentials in the mutant (V445M: -36.2 ± 0.5 mV, $n = 9$ vs. WT-hSkM1: -32.7 ± 0.8 mV, $n = 13$; $P < 0.01$). This shift in the voltage-dependence of activation along with the defect in fast inactivation are likely to be important factors responsible for myotonia associated with this mutation.

3.2. Computer simulation of V445M action potentials

Our findings reveal subtle defects in V445M gating, similar, but not identical, to other previously characterized myotonia-associated *SCN4A* mutations [11–16]. To evaluate whether the degree of dysfunction exhibited by V445M is sufficient to induce sarcolemmal hyperexcitability, we simulated skeletal muscle action potentials using a modified Hodgkin–Huxley mathematical model [10]. The rate constants for channel gating characteristics used by the model were modified to account for the behavior of the mutant (see Section 2), and simulations assumed heterozygosity for mutant and WT channels replicating the autosomal dominant transmission observed in the associated disease phenotype [6]. Fig. 3 illustrates the results of this analysis showing that only a single

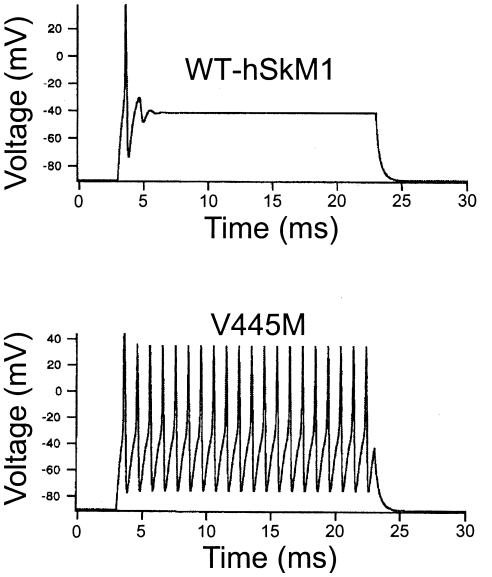

Fig. 3. Computer simulations of muscle action potential behavior for WT-hSkM1 or V445M expressing muscle fibers. Simulated membrane responses to a 20 ms, 160 μA/cm^2 stimulus at 37°C for muscle cells expressing WT-hSkM1 alone (WT) or a 1:1 ratio of WT and V445M mutant channels. Model parameters were modified as described in Section 2.

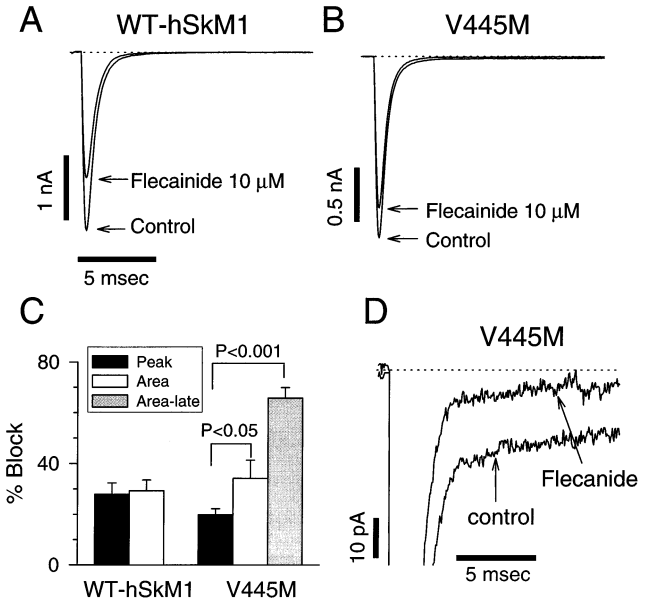

Fig. 4. Flecainide block of WT-hSkM1 and V445M. A: Sodium currents recorded from a cell expressing WT-hSkM1 during a single 100 ms test depolarization to −20 mV from a holding potential of −120 mV before (control) and after application of 10 μM flecainide. B: Effect of flecainide on currents recorded from a cell expressing V445M. C: Summarized data illustrating effects of flecainide on peak sodium current ('Peak') and the total integrated current ('Area') for both WT ($n=7$) and mutant sodium channels ($n=4$). The effect of flecainide on V445M current measured between 2.5 and 20 ms after the test depolarization ('Area-late') is also shown. D: Expanded scale of V445M non-inactivating currents before (control) and after application of 10 μM flecainide.

action potential is generated in response to a 20 ms stimulus in simulated WT muscle fibers. By contrast, modification of the model to incorporate changes in inactivation kinetics as observed with V445M results in myotonic-like repetitive action potentials. These results strongly suggest that the biophysical defect observed for V445M is sufficient to cause myotonia.

3.3. Effect of flecainide on WT and mutant sodium channels

The V445M mutation is associated with an unusual form of myotonia that is relatively refractory to the anti-myotonic compound mexiletine, but affected individuals respond dramatically to the potent sodium channel blocker flecainide [6]. Therefore we tested the effects of this compound on both WT and V445M channels. Fig. 4 illustrates the effect of 10 μM flecainide on currents elicited by a single test depolarization in cells transiently transfected with either WT-hSkM1 or V445M. Peak current amplitudes are reduced by flecainide in both WT-hSkM1 and V445M expressing cells, but the proportional decrease in the current is not significantly different between the two channel alleles. In addition to using the reduction in peak current amplitude as a measure of drug sensitivity, we also evaluated the proportional reduction in total current by comparing the area under the current traces [17] before and after application of flecainide. We observed that drug block of total current exhibited by V445M is significantly greater than block of peak current (Fig. 4C). The likely explanation for this difference is that flecainide more effectively suppresses the late current component in the mutant as compared to its effect on peak current (see 'Area-late' bar in Fig. 4C). This is illustrated further in Fig. 4D showing an expanded view of superimposed current records for the mutant before and after application of 10 μM flecainide. Although the drug concentration used in this in vitro study is higher than the therapeutic concentration, these results suggest that the beneficial effect of flecainide in patients with V445M is likely due to selective suppression of the abnormal sodium current component. Selective drug suppression of non-inactivating behavior of mutant cardiac sodium channels that occurs in the congenital long QT syndrome has been similarly observed [18].

4. Conclusions

The novel *SCN4A* mutation V445M is associated with an unusual form of mexiletine refractory, painful congenital myotonia and is caused by subtle defects in the inactivation properties of the mutant sodium channel. The observed functional disturbances including a shift in the voltage-dependence of activation to more negative potentials and the occurrence of a small non-inactivating current component, help to explain the pathogenesis of myotonia associated with the V445M mutation. Finally, the selective suppression by flecainide of the inactivation defect associated with this sodium channel allele suggests that additional studies to determine the clinical utility of this compound in treating other forms of myotonia caused by *SCN4A* mutations are warranted.

Acknowledgements: This work was supported by grants from the NIH (NS32387 to A.L.G., and HL51197 to P.B.B.), and the Muscular Dystrophy Association (P.C.R.).

References

[1] George Jr., A.L. (1996) Nephrol. Dial. Transpl. 11, 1730–1737.
[2] Chen, Q., Kirsch, G.E. and Zhang, D. et al. (1998) Nature 392, 293–296.
[3] Kohrman, D.C., Smith, M.R., Goldin, A.L., Harris, J. and Meisler, M.H. (1996) J. Neurosci. 16, 5993–5999.
[4] Rüdel, R., Ricker, K. and Lehmann-Horn, F. (1993) Arch. Neurol. 50, 1241–1248.
[5] Cannon, S.C. (1997) Neuromuscul. Disord. 7, 241–249.
[6] Rosenfeld, J., Sloan-Brown, K. and George Jr., A.L. (1997) Ann. Neurol. 42, 811–814.
[7] George, A.L., Komisarof, J., Kallen, R.G. and Barchi, R.L. (1992) Ann. Neurol. 31, 131–137.
[8] Makita, N., Bennett, P.B. and George Jr., A.L. (1996) Circ. Res. 78, 244–252.
[9] Wang, D.W., George Jr., A.L. and Bennett, P.B. (1996) Biophys. J. 70, 238–245.
[10] Richmond, J.E., VanDeCarr, D., Featherstone, D.E., George Jr., A.L. and Ruben, P.C. (1997) Biophys. J. 73, 1896–1903.
[11] Yang, N., Ji, S. and Zhou, M. et al. (1994) Proc. Natl. Acad. Sci. USA 91, 12785–12789.
[12] Hayward, L.J., Brown Jr., R.H. and Cannon, S.C. (1996) J. Gen. Physiol. 107, 559–576.
[13] Mitrovic, N., George Jr., A.L., Lerche, H., Wagner, S., Fahlke, C. and Lehmann-Horn, F. (1995) J. Physiol. (Lond.) 487, 107–114.
[14] Mitrovic, N., George Jr., A.L. and Heine, R. et al. (1994) J. Physiol. (Lond.) 478, 395–402.
[15] Lerche, H., Heine, R. and Pika, U. et al. (1993) J. Physiol. (Lond.) 470, 13–22.
[16] Lerche, H., Mitrovic, N., Dubowitz, V. and Lehmann-Horn, F. (1996) Ann. Neurol. 39, 599–608.
[17] Wang, D.W., George Jr., A.L. and Bennett, P.B. (1996) Biophys. J. 70, 1700–1708.
[18] Wang, D.W., Yazawa, K., Makita, N., George Jr., A.L. and Bennett, P.B. (1997) J. Clin. Invest. 99, 1714–1720.